APSB
Acta Pharmaceutica Sinica B

2020
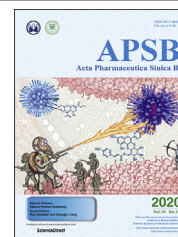
ORIGINAL ARTICLE

Lactoferrin-mediated macrophage targeting delivery and patchouli alcohol-based therapeutic strategy for inflammatory bowel diseases

Yuge Zhao[a,b,c], Yuting Yang[a,b], Jiaxin Zhang[a,d], Rong Wang[a,b], Biyun Cheng[a,c], Dipika Kalambhe[a,c], Yingshu Wang[a,d], Zeyun Gu[a,c], Dongying Chen[a,e,*], Bing Wang[a,*], Yongzhuo Huang[a,c,f,g,*]

[a]*State Key Laboratory of Drug Research, Shanghai Institute of Materia Medica, Chinese Academy of Sciences, Shanghai 201203, China*
[b]*Nanchang University College of Pharmacy, Nanchang 330006, China*
[c]*University of Chinese Academy of Sciences, Beijing 100049, China*
[d]*Shanghai University of Traditional Chinese Medicine, Shanghai 201203, China*
[e]*Laboratory of Pharmaceutical Analysis, Shanghai Institute of Materia Medica, Chinese Academy of Sciences, Shanghai 201203, China*
[f]*NMPA Key Laboratory for Quality Research and Evaluation of Pharmaceutical Excipients, Shanghai 201203, China*
[g]*Zhongshan Branch, The Institute of Drug Research and Development, Chinese Academy of Sciences, Zhongshan 528437, China*

Abstract Inflammatory bowel diseases (IBD) are the incurable chronic recurrent gastrointestinal disorders and currently lack in safe and effective drugs. In this study, patchouli alcohol, a main active compound of traditional Chinese herb patchouli, was developed into biomimetic liposomes for macrophage-targeting delivery for IBD treatment. The developed lactoferrin-modified liposomes (LF-lipo) can specifically bind to LRP-1 expressed on the activated colonic macrophages and achieve cell-targeting anti-inflammatory therapy. LF-lipo reduced the levels of inflammatory cytokines and ROS and suppressed the MAPK/NF-κB pathway. LF-lipo also suppressed the formation of NLRP3 inflammasome and the consequent IL-1β activation. LF-lipo showed improved therapeutic efficacy in a DSS-induced colitis murine model, evidenced by the reduced disease activity index, the improved colon functions, and the downregulated inflammatory cytokines in the colon. LF-lipo provided an effective and safe macrophage-

*Corresponding authors.
E-mail addresses: dychen@simm.ac.cn (Dongying Chen), bwang@simm.ac.cn (Bing Wang), yzhuang@simm.ac.cn (Yongzhuo Huang).

targeting delivery and therapeutic strategy for addressing the unmet medical need in IBD management.

1. Introduction

Inflammatory bowel diseases (IBD), mainly divided into Crohn's disease (CD) and ulcerative colitis (UC), are characterized by chronic inflammation in the gastrointestinal tract that can lead to long-term and even irreversible damage[1]. IBD are common in North America and Europe, with the highest incidence in the developed and urbanized areas[2]. In the past score years, the incidence of IBD has dramatically been elevating in developing countries; for instance, it is expected that there will be 1.5 million IBD patients in China by 2025[3]. The etiology and pathogenesis of IBD might be related to genetic susceptibility, impaired intestinal mucosal barrier function, and immune homeostasis disorders[4−6], but still largely remains unknown. Current drug therapy includes salicylate, corticosteroids, and immunosuppressants, but yields limited outcomes, with poor response rate[7]. In addition, patients often suffer from serious complications and poor prognosis, such as infectious diseases and a high incidence of cancer[8]. Therefore, it is an urgent need for seeking a novel therapeutic strategy.

Traditional herbs have been used for hundreds of years for treating colitis in China[9], and actively been investigated to identify the active compounds[10]. For example, a herb Guang Huo Xiang (*Pogostemon cablin (Blanco)* Benth.) has been in a long-standing clinical practice for gastrointestinal diseases, and its active compound, patchouli alcohol (or patchoulol, PA), a tricyclic sesquiterpenoid, has been recently revealed with the functions of suppressing the NF-κB-mediated intestinal inflammation[11]. The therapeutic value of PA was demonstrated in various animal models of inflammation[12,13]. Therefore, PA is a potential drug candidate for IBD treatment.

Macrophages play a bi-directional role in the initiation, progression, and regression of inflammation[14]. M1-subtype macrophages are pro-inflammatory, with an important effect on the host defense against infection, while M2 is associated with anti-inflammatory responses and tissue repair[15]. Macrophage modulation is an important therapeutic strategy for some complicated diseases like IBD and cancer[16,17]. There is little known about the macrophage regulation effect of PA and such an application on IBD therapy.

PA is water-insoluble and difficult to formulate into a conventional dosage form. Oral delivery of PA is restricted by the poor bioavailability. Currently, there have been few PA advanced drug delivery systems reported for systemic administration. In this study, we designed a lactoferrin-modified liposome (LF-lipo) for delivering PA to colonic macrophages for anti-inflammatory activity. Lactoferrin serves as an important nutrient carrier that transfers iron to the cells. Importantly, lactoferrin can specifically bind to low-density lipoprotein receptor-related protein (LRP-1) that is expressed on the inflammatory macrophages and serves as an endogenous regulator of macrophage[18,19]. Therefore, the lactoferrin modification conferred the biomimetic delivery function to the liposomes. Similar to tumor tissues, the inflamed intestinal tissues are also characterized by the epithelial enhanced permeability and retention (eEPR) effect that benefits the nanomedicine treatment, due to defective architecture of the vessel walls[16]. Therefore, it was expected that the biomimetic LF-lipo could achieve both active and passive targeting delivery to inflamed colonic tissues.

2. Materials and methods

2.1. Materials

Lactoferrin (Jingruijiuan Biotechnology Co., Ltd., Nanjing, China). Patchouli alcohol (PA, Manster Biotechnology Co., Ltd., Chengdu, China). DSPE-PEG-NHS, DSPE-PEG$_{2000}$, egg yolk lecithin (PC-98T), and cholesterol (Advanced Vehicle Technology Co., Ltd., Shanghai, China). Rabbit LRP-1 monoclonal antibody, murine GAPDH monoclonal antibody, and Actin monoclonal antibody (Abcam, Cambridge, UK). Cocktail and lipopolysaccharides (LPS, Sigma−Aldrich, St. Louis, MI, USA). Horseradish peroxidase (HRP)-conjugated goat anti-rabbit/mouse lgG secondary antibody (Beyotime, Shanghai, China). Cytokines (Peprotech, Rocky Hill, NJ, USA). RNA extraction reagent and RNA reverse transcription kit (Yisheng Biotechnology, Shanghai, China). Other reagents of analytical grade (Sinopharm Chemical Reagent Co., Ltd., Shanghai, China).

2.2. Cells and animals

The bone marrow-derived macrophages (BMDM) were prepared from bone marrow-derived monocytes from BALB/c mice using a standard protocol. In brief, BMDM was induced in the DMEM medium containing 20% FBS and 20 ng/mL M-CSF. M1 subtype was differentiated using 100 ng/mL LPS and 20 ng/mL IFN-γ cytokine, while M2Φ using 40 ng/mL IL-4.

BALB/c female mice (about 8 weeks) were obtained from Shanghai Laboratory Animal Center, Chinese Academy of Sciences, China. Animal experiments were performed following the Institutional Animal Care and Use Committee (IACUC) guidelines and approved by the Shanghai Institute of Materia Medica (SIMM), Chinese Academy of Sciences, Shanghai, China.

2.3. Preparation of LF-lipo

The liposomes were fabricated by using a standard thin-film method. In brief, lecithin yolk, cholesterol, DSPE-PEG$_{2000}$, DSPE-PEG-NHS (30:6:6:1, *w/w*), and patchouli alcohol were proportionally weighed and dissolved in chloroform. Chloroform was removed under vacuum using a rotary evaporator. PBS was

added to hydrate the dry lipid film to form an aqueous liposome suspension. The liposomes were processed by an ultrasonic probe. The liposomes were pushed through the polycarbonate membrane with the use of an extruder (Avanti Polar Lipids, Alabaster, AL, USA) and then purified using a Sephadex G-50 column (GE Healthcare, Boston, MA, USA) to get rid of free patchouli alcohol. LF (8 mg) was added to the liposome suspension for incubation overnight. The thus-formed LF-lipo was further purified. Free lactoferrin was removed by centrifugation using an Amico filter device (100 K, MilliporeSigma, Burlington, MA, USA).

2.4. Characterization of LF-lipo

The LF modification content in the liposome was analyzed by SDS-PAGE, and measured by using ImageJ software (https://imagej.nih.gov). Particle size, polydispersity index (PDI), and ζ-potential were determined by Zeta Size Nanoparticle Analyzer (Malvern Panalytical, Malvern, UK). The liposomes were imaged by transmission electron microscopy (TEM). The drug-loading capacity (DL, %) and entrapment efficiency (EE, %) were determined by GC-FID (Agilent 6890N, Agilent Technologies, Santa Clara, CA, USA).

2.5. Stability and in vitro drug release

Liposome samples were suspended in PBS containing 10% FBS and placed on a shaker at 37 °C. Particle size change was monitored at a preset time course. Drug accumulative release was performed by placing liposomes in a dialysis tube in a PBS release medium (pH 7.4) containing 15% ethanol at a sink condition. The experiment was conducted at a shaker (37 °C, 150 rpm), Suzhou Pei-Ying Experimental Instrument Co. Ltd., Taichang, China) and, at various time points, 0.5 mL of the release medium was sampled and equal volume of fresh medium supplemented. The PA concentration at the released medium was determined by GC-FID.

2.6. Cellular uptake assay

M1Φ or HUVEC were treated with the coumarin-6-labeled LF-lipo for 1 h and then washed thoroughly. In the blockade study, the M1Φ were pretreated with 50 μmol/L lactoferrin to block LRP-1 for 1 h followed by incubation with LF-lipo. The intracellular delivery efficiency was measured by a flow cytometer (FACS Calibur, Becton Dickinson, Franklin Lakes, NJ, USA). The cells were fixed with 4% paraformaldehyde and stained with DAPI and observed with fluorescence microscopy (CARL ZEISS, Oberkochen, Germany).

2.7. Cell viability assay

The cytotoxicity of the drugs to macrophages was measured by a standard MTT assay. M1Φ were cultured with different concentrations of PA, Lipo, and LF-lipo for 24 h, followed by MTT procedures. The absorbance at 490 nm was recorded by a microreader (Multiskan, Thermo Fisher, Waltham, MA, USA).

2.8. Cytokine analysis by ELISA

The levels of cytokines were measured using an ELISA kit (Dakewe, Beijing, China) following a protocol from the manufacturer.

2.9. Cytokine analysis by qPCR

RNA extracted from the macrophages or tissues was used to process RNA-to-cDNA transcription using a reverse transcription kit for quantitative PCR according to a standard protocol. The amplification was processed for 1 cycle at 95 °C for 5 min and 40 cycles at 95 °C (10 s), 60 °C (20 s), and 72 °C (20 s).

2.10. Western blot

Proteins in cells or tissues were extracted using a radio-immunoprecipitation assay (RIPA) lysate kit and the concentration measured by a BCA protein assay kit (Beyotime, Shanghai, China). The samples were then processed by SDS-PAGE and electrophoretically transferred onto a polyvinylidene fluoride membrane that subsequently was blocked with 5% BSA solution for 1 h and then sequentially treated with the intended primary antibodies and HRP-labeled secondary antibody. The membrane was subjected to a ChemiDoc MPTM Imaging System (Bio-Rad, Hercules, CA, USA).

2.11. Measurement of intracellular ROS

Macrophages in 12-well plates were exposed to PA, Lipo, or LF-lipo for 12 h, respectively, to detect the intracellular ROS level. Then cells were analyzed using a ROS detection kit (Beyotime, Shanghai, China) and a flow cytometer.

2.12. Biodistribution study by in vivo imaging

Intravenous administration of Cy5-labeled LF-lipo or Lipo was given to the colitis mice. The biodistribution of the LF-lipo and Lipo was analyzed using the IVIS imaging system (Caliper PerkinElmer, Hopkinton, USA) at a preset time course. At the endpoint, the mice were sacrificed, and the organs including the colon were dissected for ex vivo imaging.

2.13. Targeting colonic macrophage study

The colitis model mice were intravenously injected with the Cy5-labeled LF-lipo or Lipo. After 24 h, the mice were euthanized and the colon tissues were dissected to prepare the cell suspension. CD45, CD11b, F4/80, and CD86 antibodies were used for cell staining and M1Φ sorting. Flow cytometry was used to screen M1Φ containing Cy5-liposomes (CD86^{+}/Cy5^{+}).

2.14. DSS-induced colitis in mice

The colitis model induced by DSS was established according to a previous method[20]. The mice were given a three-cycle DSS treatment to induce chronic colitis, each containing 7-day 2% DSS and then 14-day drinking water. Following this pattern, the mice underwent three cycles to induce chronic colitis. The colitis animals were randomly set into a DSS group (untreated control) and three treatment groups (i.e., PA, Lipo, and LF-lipo), while a healthy group as a control. Drug therapy was given at each interval of the cycle via intravenous injection at a PA dose of 15 mg/kg.

2.15. Evaluation of colitis treatment efficacy

During the treatment period, body weight changes, visible stool consistency, and fecal bleeding were assessed daily for
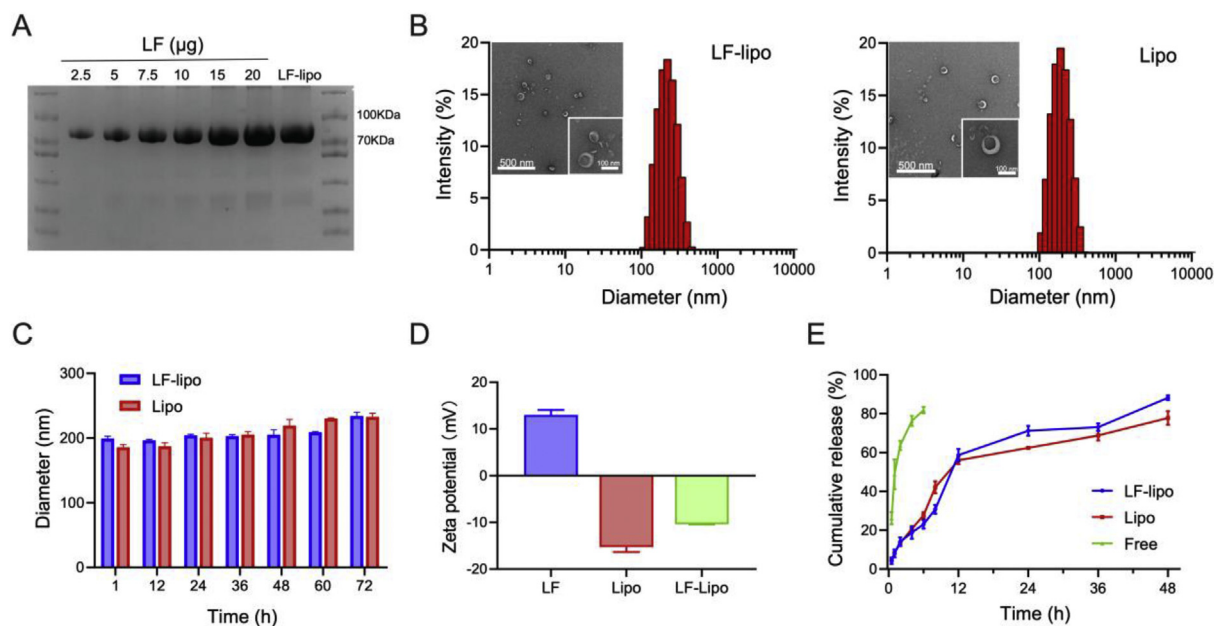
Figure 1 Characterization of LF-lipo. (A) LF modification ratio in LF-lipo detected by Coomassie brilliant blue staining in SDS-PAGE electrophoresis. (B) Particle size and TEM images of LF-lipo and Lipo. (C) Stability of LF-lipo and Lipo in a serum-containing PBS. (D) ζ-potential measurement. (E) *In vitro* release of PA from LF-lipo and Lipo. Data are expressed as mean ± SD ($n = 3$).

determining disease activity index (DAI) that serves as the summation of the stool consistency index (0−3), fecal bleeding index (0−3), and weight loss index (0−4)[21]. After treatments, the colonic length (from the cecum to the rectum) was determined. The distal section was dissected to analyze the cytokines and related biomarkers. The dissected organs were weighed, and processed for histological examination.

2.16. Analysis of intestinal permeability

After fasting for 24 h, the colitis mice were given FITC-Dextran (100 mg/mL in PBS) with a dose of 44 mg/100 g *via* intragastric administration. After 4 h, blood was sampled from the orbit, and the serum concentration of FITC-Dextran was detected at λ 485 nm.

2.17. Analysis of colonial immune cells

The procedure was modified from a previous report[22]. Colon tissues were dissected, opened longitudinally, and then incubated with HBSS solution containing DTT and EDTA. The mucus was washed away with cold PBS. Colon tissues were cut into 1-cm pieces for enzymatic digestion (RPMI, 2% FBS, 200 U/mL collagenase type IV) at 37 °C for 1 h. The cell suspension prepared from the homogenized tissues was incubated with the target antibodies for flow cytometric assay.

2.18. Statistical analysis

T-test and one-way ANOVA were used for statistical analysis. Data are presented as mean ± standard deviation (SD). *n* value was 3, if it was not specified. Statistical differences were defined as $^{*}P < 0.05$, $^{**}P < 0.01$, and $^{***}P < 0.001$; ns means not significant.

3. Results

3.1. Characterization of lactoferrin-modified liposomes (LF-lipo)

LF-lipo was prepared using a typical thin-film method as reported previously[23]. The lactoferrin/DSPE-PEG-NHS conjugation efficiency in the liposome was 13.3% (*mol/mol*, Fig. 1A). The particle size of LF-lipo and Lipo was about 140 nm (Fig. 1B) with a polymer dispersity index (PDI) around 0.2 (Supporting Information Table S1). They maintained colloidal stability for 72 h in PBS containing 10% FBS (Fig. 1C). The LF-lipo and Lipo were negatively charged (Fig. 1D). The drug-loading capacity (DL %) and entrapment efficiency (EE%) were listed in Table S1. Both liposomes show a slow release profile in a PBS containing 15% ethanol (Fig. 1E). It should be noted that ethanol was used to increase PA solubility in PBS to ensure sink condition.

3.2. Cellular uptake assay

LF-lipo was designed for targeting LRP-1 on the macrophages. The LRP-1 expression was high in M1 macrophages (M1Φ) and the colonic tissues, but low in normal tissues, HUVEC cells, and M2Φ (Fig. 2A). M1-associated biomarkers (iNOS, STAT1) were highly expressed in the inflammatory colons, while the M2-related mannose receptor was poorly expressed. It suggests that the M1 subtype was the dominant subpopulation of macrophages in the inflammatory colons. The cellular uptake efficiency of LF-lipo was 2.2-fold higher than the non-modified Lipo (Fig. 2B and C). When the cells were pretreated with lactoferrin to block LRP-1, the uptake of LF-lipo decreased to the same level as that of Lipo (Fig. 2C and D). Meanwhile, there was no significant difference between LF-Lipo and Lipo in the uptake by HUVEC with poor expression of LRP-1 (Supporting Information Fig. S1); the result is also supported by confocal microscopic imaging
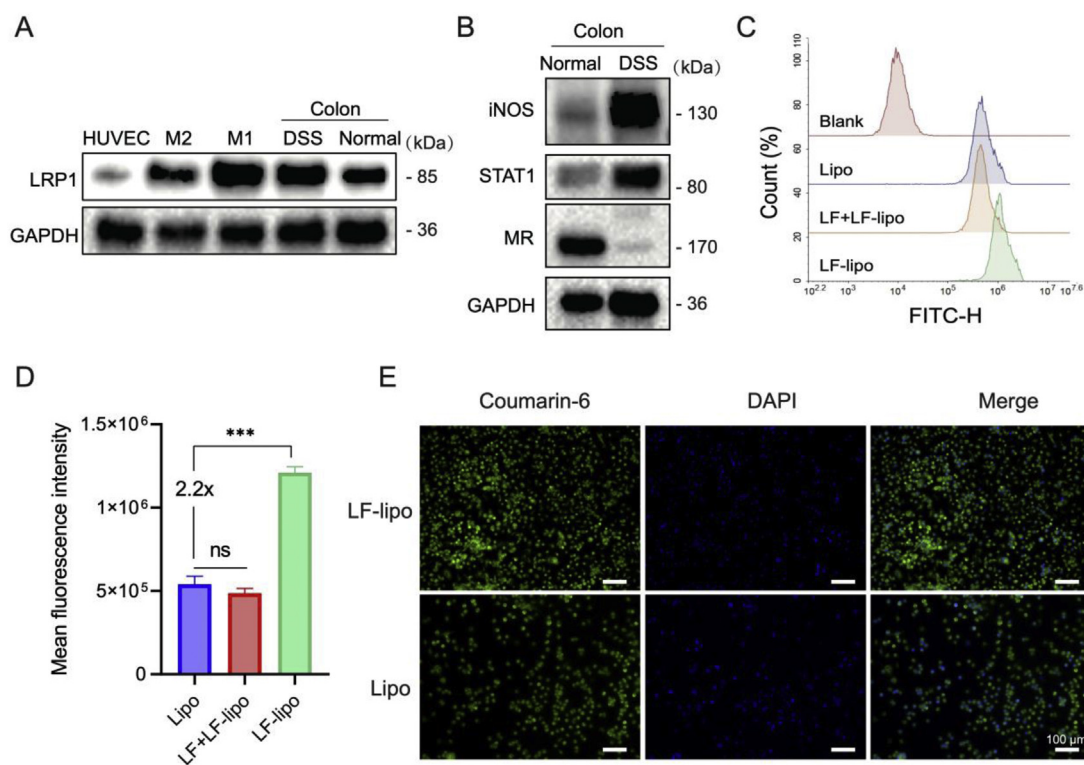
Figure 2 Cellular uptake of LF-lipo and Lipo. (A) Expression of LRP-1 on HUVEC cells, macrophages, and colonic tissues. (B) M1 and M2Φ in the normal and DSS-induced colitis tissues detected by Western blot (M1 markers: iNOS, STAT1; M2 marker: MR). Flow cytometric assay of cellular uptake efficiency in M1Φ (C) and statistical analysis (D). (E) Confocal fluorescence images of M1Φ after incubation with coumarin-6-labeled LF-lipo and Lipo (scale bar = 100 μm). Data are expressed as mean $\pm$ SD ($n = 3$). $^{***}P < 0.001$; ns, no significance.

(Fig. 2D). It suggests the importance of LF/LRP-1 interaction in mediating M1Φ-targeting delivery.

3.3. M1Φ regulation by LF-lipo

M1Φ are the inflammatory immune cells that generate and release large amounts of inflammatory cytokines and trigger the inflammatory responses. By contrast, M2Φ possess anti-inflammatory functions and heal the impaired tissues. After treatment with PA, LF-lipo, or lipo, the mRNA levels of the pro-inflammatory cytokines including *IL-1β, IL-6, IL-12, IL-18, and TNF-α* in the M1Φ were significantly reduced, and LF-lipo had the best effect (Fig. 3A). After drug treatment, the secreted cytokines by the M1Φ in the supernatants were measured by ELISA, and LF-lipo also remarkably suppressed the secretion of the proinflammatory IL-1β, IL-6, IL-12, and TNF-α (Fig. 3B). By contrast, the anti-inflammatory cytokines IL-10 and TGF-β were upregulated as shown in the qPCR results (Fig. 3C). The downregulation of the inflammatory IL-1β was further confirmed by the Western blot results, while the anti-inflammatory TGF-β was up-regulated after LF-lipo treatment (Fig. 3D). Of note, the levels of CD206 and Arg-1 (the M2-associated biomarkers) were increased after LF-lipo treatment (Supporting Information Fig. S2), suggesting the repolarization from M1 to M2.

Importantly, both free drug and liposomes show high biosafety to macrophages at the tested concentrations up to 32 μg/mL (Fig. 3E), indicating that the anti-inflammatory effect of PA and liposomes on macrophages relied on repolarization, instead of M1Φ depletion.

3.4. Reduced intracellular ROS levels by LF-lipo

In addition to the effect of M1→M2 repolarization, PA is of antioxidant capacity and can restore the activity of antioxidant enzymes and thus possessed a strong free radical scavenging ability[24]. M1Φ can produce a surplus amount of reactive oxygen species (ROS) that further aggravates the immune responses by mediating secretion of pro-inflammatory cytokines IL-1β, IL-6, and TNF-α, *via* a mechanism of ROS-dependent MAPK signaling[25]. Our results show that drug treatment decreased ROS production in M1Φ and LF-lipo exhibited the most potent effect (Fig. 4A and B). Accordingly, the prof-inflammatory cytokine secretion was attenuated as shown in the section above.

3.5. The MAPK and NF-κB pathways suppressed by LF-lipo

MAPK and NF-κB are the essential inflammatory signaling pathways. The MAPKs family, including ERK, P38, and JNK, plays an important role in inflammatory signaling[26]. The activated MAPKs can trigger inflammatory responses and produce a large amount of inflammatory cytokines. It was found that the MAPK pathway activation was suppressed by LF-lipo, as reflected by the downregulation of the phosphorylated ERK, P38, and JNK (Fig. 4C).

NF-κB P65 normally binds to its inhibitor IκBα, but once stimulated by inflammatory factors (*e.g.*, LPS), IκBα degrades, thereby removing the inhibition of NF-κB P65. NF-κB P65 is subsequently phosphorylated and initiates the production of inflammatory cytokines, thus activating NF-κB/NLRP3/IL-1β
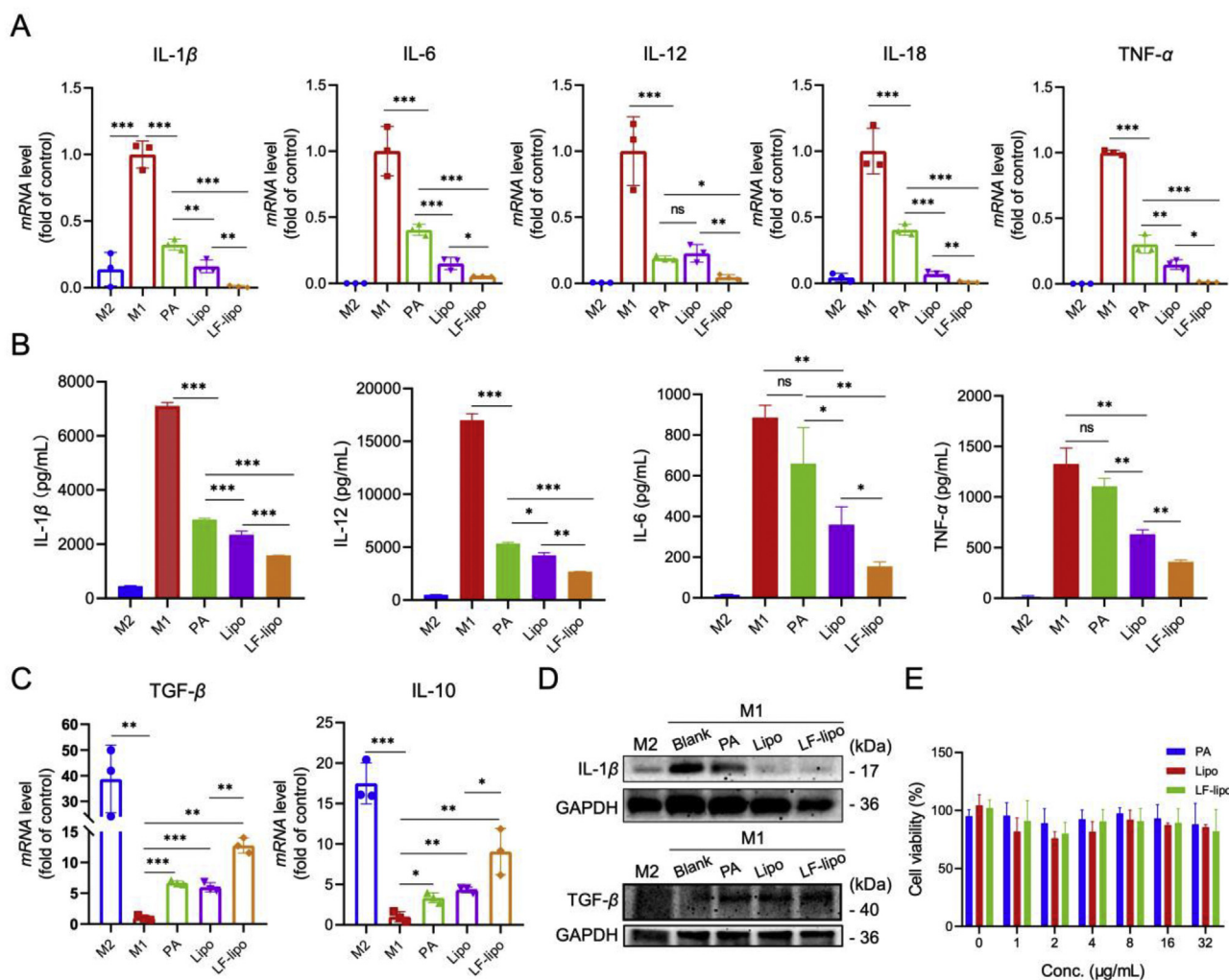
Figure 3 Macrophage regulation effect of liposomes (A) The mRNA levels of proinflammatory cytokines in the drug-treated M1Φ examined by qPCR (B) The macrophage secretory proinflammatory cytokines examined by ELISA (C) The mRNA levels of anti-inflammatory cytokines in the drug-treated M1Φ (D) The expression levels of IL-1β and TGF-β in the drug-treated M1Φ (E) The biocompatibility of liposomes with M1Φ. Data are expressed as mean $\pm$ SD ($n = 3$). $^*P < 0.05$, $^{**}P < 0.01$, $^{***}P < 0.001$; ns, no significance.

pathways: the activated NF-κB promotes the formation of NLRP3 inflammasome that consequently converts pro-IL-1β to IL-1β[27−29]. The suppression of MAPK and NF-κB pathways by LF-lipo was investigated. Our results revealed that LF-lipo efficiently inhibited IκBα degradation and NF-κB P65 phosphorylation (Fig. 4D). As a consequence, NLRP3 formation was reduced, and thereby conversion of IL-1β from pro-IL-1β was inhibited (Fig. 4E). The observation above demonstrated that the inflammation regression caused by LF-lipo treatment was associated with the MAPK and NF-κB pathways.

3.6. Biodistribution and targeting delivery of LF-lipo

The distribution and targeting effect of LF-lipo in a colitis mouse model was investigated. The results show the increased drug accumulation in the abdominal cavity in the colitis mice treated with LF-lipo (Fig. 5A and B). In the dissected colon tissues, LF-lipo had a higher accumulation than the Lipo group, because of LF-mediated targeting to the overexpressed LRP-1 in colon tissues (Fig. 5C and D).

In order to detect the uptake of Cy5-labeled LF-lipo by the colonic macrophages, flow cytometry was used to measure the CD86$^+$/Cy5$^+$ macrophages in colon tissues. There was a 2.5-fold of more CD86$^+$/Cy5$^+$ macrophages in the LF-lipo group than the Lipo group (Fig. 5E and F), demonstrating that LF-lipo exhibited enhanced efficiency targeting the M1Φ in the colon.

3.7. In vivo treatment study

The treatment study was carried out in the DSS-induced colitis mice (Fig. 6A). After drug treatment, the disease activity index (DAI, Fig. 6B) was decreased and so was the body weight loss (Fig. 6C). It indicated the improvement of the pathological conditions. LF-lipo exhibited the best treatment outcomes. The colon length was a key indicator of the colitis conditions. The colons in the untreated colitis mice were significantly shortened compared to those in the normal animals (i.e., PBS group), while the colons in the treatment groups were longer than the untreated colitis group (Fig. 6D), indicating the improvement. Colitis is characterized by enhanced intestinal permeability and orally administered FITC-dextran is an indicator for evaluating the intestinal
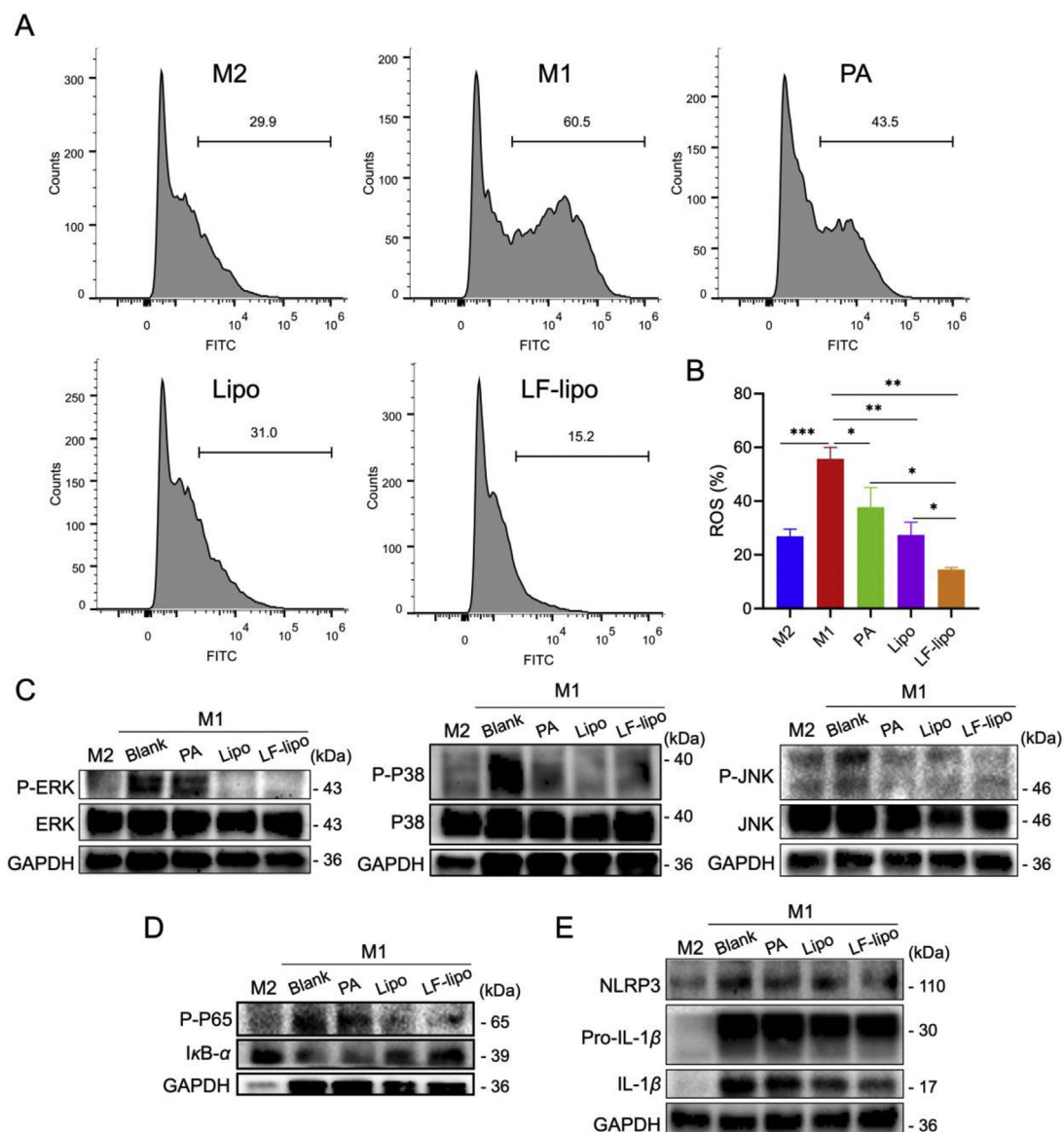
Figure 4 Anti-inflammation mechanisms of LF-lipo *via* suppressing intracellular ROS generation and the MAPK and NF-κB pathways. (A) The reduced intracellular ROS levels in M1Φ after drug treatment. (B) Statistical analysis of ROS levels. (C) The suppressed of MAPK pathway indicated by the down-regulation of P-ERK, P-P38, and P-JNK. (D) Western blot assay of NF-κB (P-P65 and IκBα) expression. (E) The down-regulation of NLRP3, Pro-IL-1β, and IL-1β in M1Φ after treatment. Data are expressed as mean $\pm$ SD ($n = 3$). $^{*}P < 0.05$, $^{**}P < 0.01$, $^{***}P < 0.001$.

permeability. As shown in the untreated colitis group, the FITC-dextran concentration in the blood obviously elevated compared to the treatment groups. However, the intestinal permeability was repaired in the treatment groups and LF-lipo treatment showed the lowest FITC-dextran concentration (Fig. 6E). The cytokine mRNA expression in the animal colon tissues were measured by qPCR, and they were significantly down-regulated after treatment, with the best effect in the LF-lipo group (Fig. 6F). Statistical analysis shows that the major factors (*e.g.*, colon length, IL-1β, and IL-6) are statistically different between LF-lipo and Lipo. The quantity of infiltrating cells in the colon tissues was measured by flow cytometry. The data indicate that the number of regulatory T cells (Tregs) in the colon increased (Fig. 6H, and Supporting Information Fig. S3), while the dendritic cells (DCs) decreased (Fig. 6I, and Supporting Information Fig. S4), especially in the

LF-lipo group. Treg cells are a pivotal suppressor of immune activation to prevent excessive inflammation[30], and Treg cells can yield a therapeutic effect on the severe inflammatory colitis[31]. Colonic lamina propria DCs are the important activator of T cells and closely associated with colitis development[32].

The treatment biosafety was preliminarily evaluated by organ coefficient measurement and histopathological examination. There is no significant difference in the organ coefficients and no pathological changes in the major organs after treatment (Fig. 7A and B).

4. Discussion

PA is a major active compound in patchouli and its extract patchouli oil that serves as herbal medicine and food supplement.
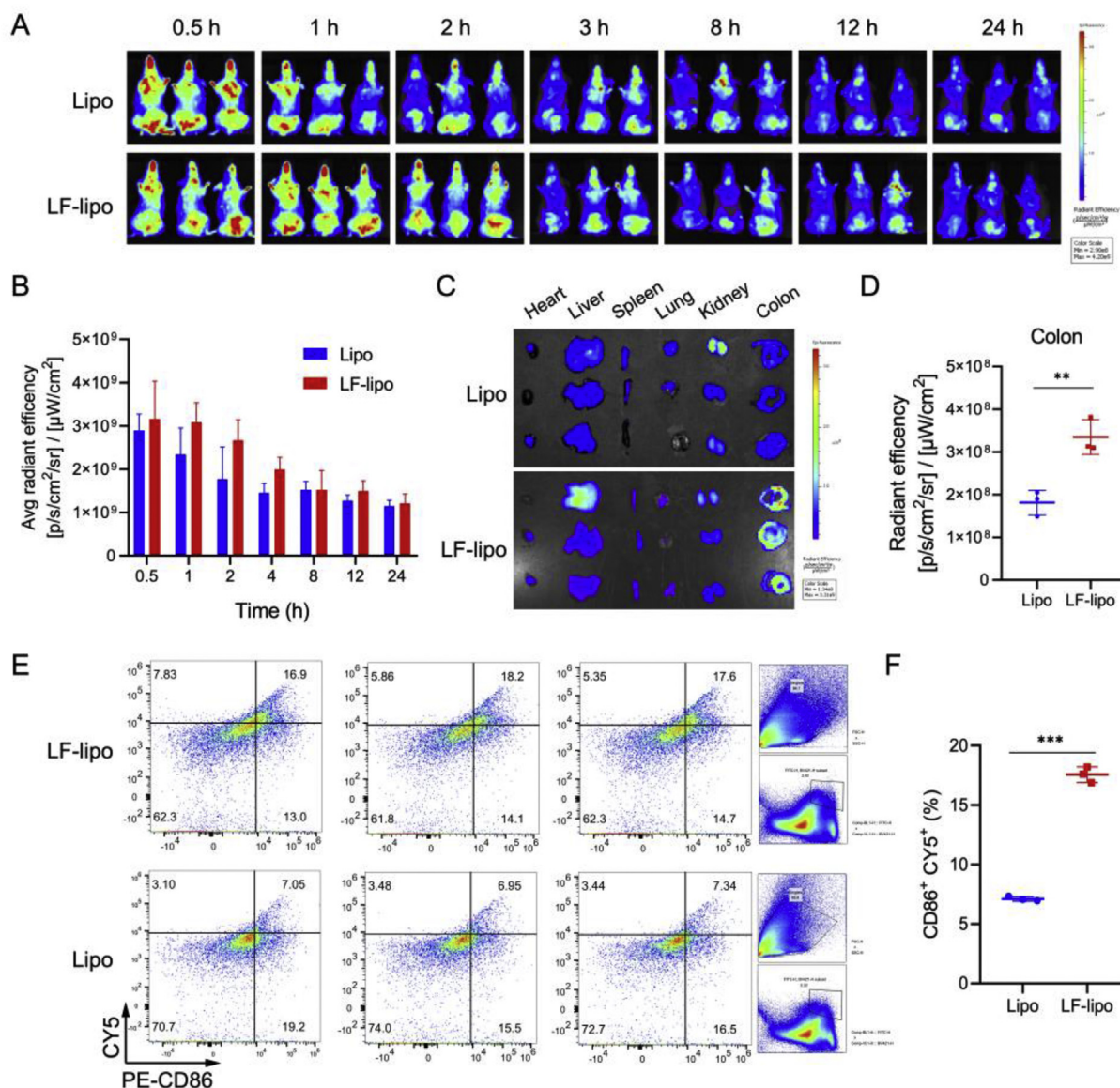
Figure 5 Biodistribution and targeting delivery study. (A) *In vivo* imaging of colitis mice. (B) Statistical analysis of *in vivo* radiant efficiency. (C) *In vitro* radiant efficiency of the major organs and colons. (D) Statistical analysis of *ex vivo* colonic radiant efficiency. (E) M1Φ-tageting evaluation by detecting the M1 that captured Cy5 labeled liposomes in colitis tissues, indicated by population of CD86$^+$/Cy5$^+$ macrophages detected by flow cytometry (F) Statistical analysis of CD86$^+$Cy5$^+$ macrophage population. Data are expressed as mean ± SD ($n = 3$). $^{**}P < 0.01$, $^{***}P < 0.001$.

PA is safe and the maximum dose in animal studies can reach 100 mg/kg *via* oral administration[33]. PA is involved in various therapeutic purposes, *e.g.*, anti-inflammation[11], anti-atherosclerosis[34], anti-influenza virus infection[35], and antibacterial infection[36]. The common therapeutic target of these applications is macrophages. In the intestinal mucosa, macrophages are bountiful and predominately involved in IBD, and the activated M1 subgroup of macrophages is an essential inflammatory mediator driving the inflammation progression[37]. Therefore, PA-based macrophage modulation and anti-inflammatory treatment have attracted much attention due to its efficacy and safety. Yet, its low bioavailability imposes a challenge against the clinical translation.

Inflammation targeting delivery has been actively studied[38]. Although there have been some works on inflamed colon targeting delivery, the target delivery to an inflamed cell type (*e.g.*, M1Φ) in

colitic tissues is still under-explored. LRP-1 is highly expressed in inflamed macrophages and is related to the inflammation[39,40]. But currently, there was no report about the potential of LRP-1 as a drug delivery target for colitis treatment. Our work used LF as a targeting ligand for colitis-targeting delivery, and its natural receptor is LRP-1. In recent years, the EPR-based targeting mechanism has been under bitter debate for the applicability in cancer therapy due to the high heterogenicity of tumors[41]. But its application in inflammatory diseases (*i.e.*, eEPR effect) has drawn more and more attention[42,43]. Increased vessel permeability and vascular leak are common in the inflammatory tissues[44]. Nano drugs *via* systemic administration can efficiently accumulate in the inflamed and damaged tissues through the eEPR effect[45]. The biodistribution efficiency in the inflammatory colon tissues is associated with particle size; for example, the nanoparticles around 110 nm was better than the smaller 50 nm and the larger
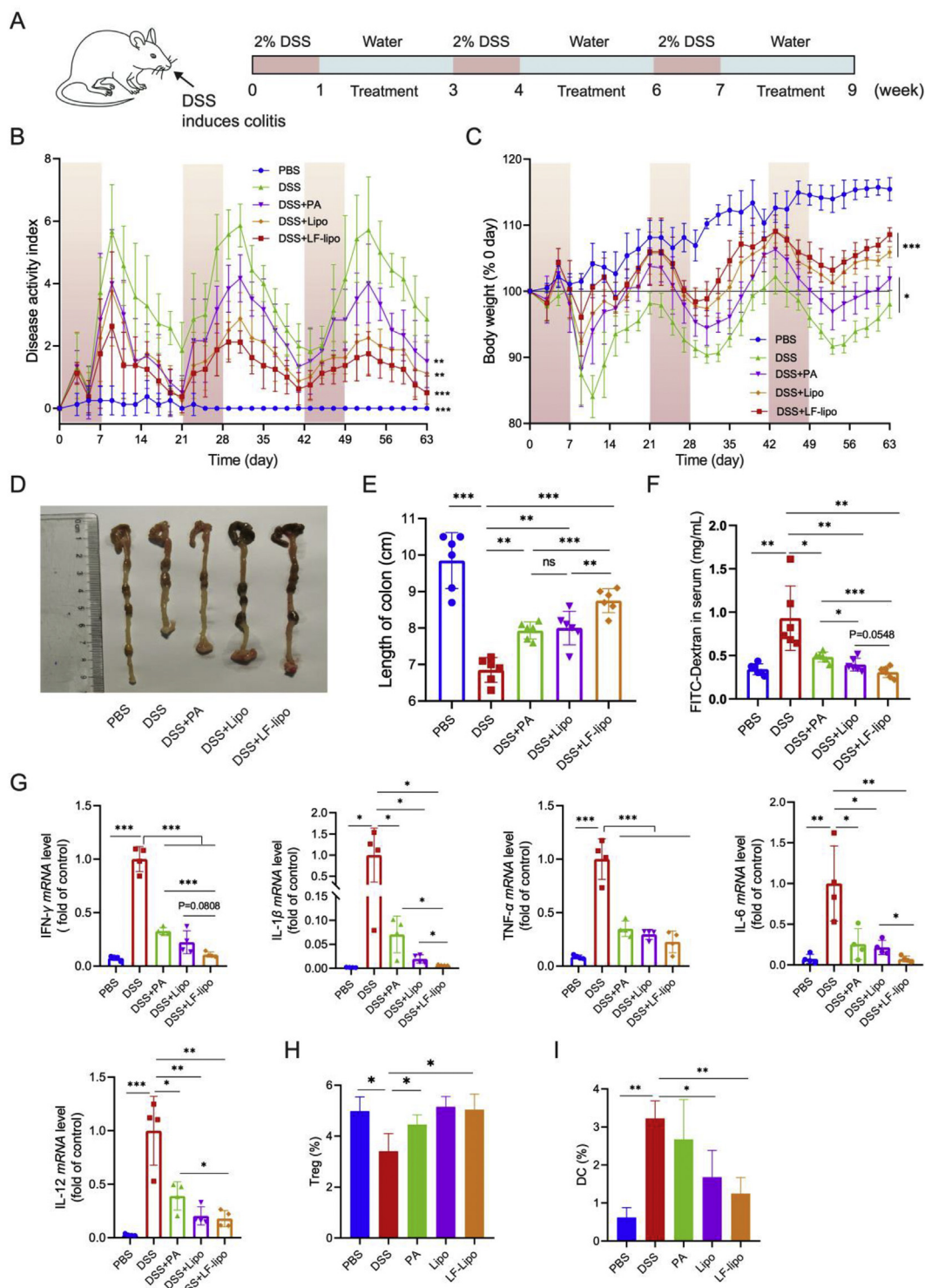
Figure 6 *In vivo* treatment study. (A) Schematic diagram of colitis induction and treatment. (B) Disease activity index (DAI) record. (C) Changes in body weight during the treatment. (D) Representative colon tissues of each group. (E) Statistical analysis of colon length. (F) Intestinal permeability indicated by serum FITC-Dextran concentration. (G) Cytokines in the colons detected by qPCR. Population of Tregs (H) and DCs (I) in colon tissues. Data are expressed as mean ± SD (B, C, E, F, G, $n = 6$; H, I, $n = 3$). $^*P < 0.05$, $^{**}P < 0.01$, $^{***}P < 0.001$; ns, no significance.

180 nm[46]. In addition, there are a large number of macrophages infiltrating into the inflamed colon, providing a great advantage of facilitating the uptake of nanoparticles into the inflammatory macrophages. Therefore, nanomedicine is promising for IBD therapy *via* systemic administration.

It is well accepted that macrophages are an important drug target of IBD treatment[47]. NF-κB signaling in the macrophages triggers inflamed responses, and NF-κB upregulation in the inflamed tissues was found in the UC patients[48]. The MAPK signaling activation is common in the inflammatory macrophages
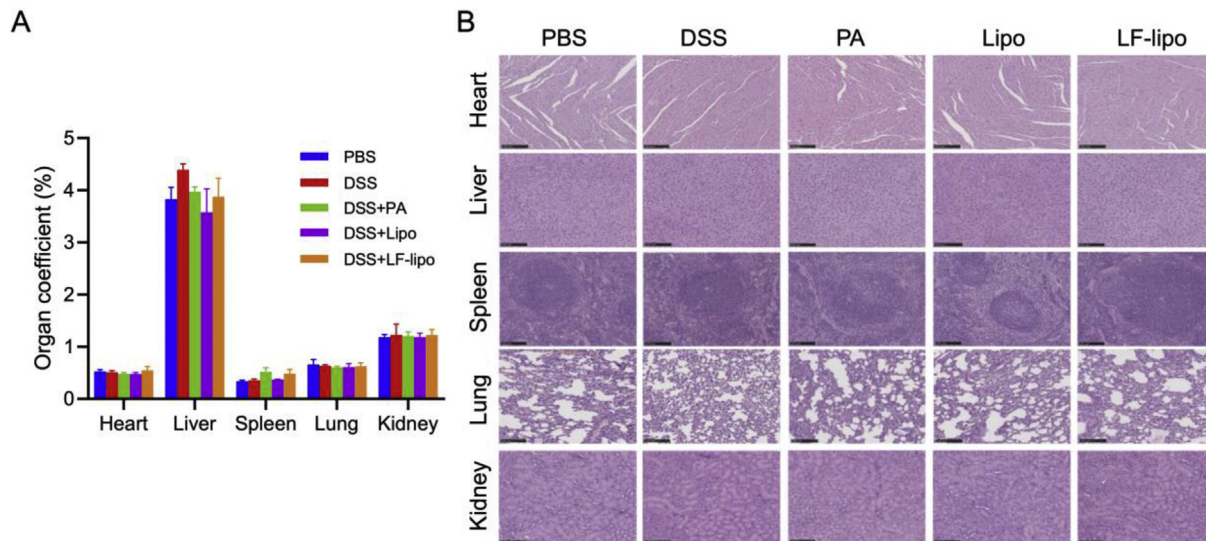
Figure 7 Preliminary biosafety evaluation. (A) Organs coefficients; there was no signficant difference among the groups. (B) The histological examination of the major organs (scale bar = 100 μm). There were no pathological changes. Data are expressed as mean ± SD ($n = 6$).

and colitis tissues[49]. Therefore, a therapeutic strategy for suppression of the MAPK/NF-κB pathway may improve inflammatory diseases, such as colitis[50]. Our work demonstrated that PA could inactivate MAPK and NF-κB and repolarize the inflammatory M1Φ to the anti-inflammatory M2 subtype.

5. Conclusions

A macrophage-targeting therapeutic method and a liposomal delivery strategy were designed for IBD in this work. LF was applied as a liposomal ligand for targeting delivery to the inflammatory macrophages at the lesion site. The targeting effect of LF-lipo was verified by the *in vitro* and *in vivo* experiments. LF-lipo can reduce the production of ROS and downregulate inflammatory cytokines. The anti-inflammatory mechanisms were related to inhibiting MAPK/NF-κB pathway. LF-lipo exhibited enhanced treatment outcomes in a colitis murine model. This study provides a safe and effective therapeutic method for IBD management.

Acknowledgments

Author contributions

Yongzhuo Huang, Bing Wang, Dongying Chen designed the research and performed data analysis. Yuge Zhao, Yuting Yang, Jiaxin Zhang, Rong Wang, Dipika Kalambhe, Yingshu Wang and Zeyun Gu carried out the experiments. Yongzhuo Huang and Yuge Zhao wrote the manuscript. All of the authors have read and approved the final manuscript.

Conflicts of interest

The authors have no conflicts of interest to declare.

Appendix A. Supporting information

Supporting data to this article can be found online at https://doi.org/10.1016/j.apsb.2020.07.019.

References

1. Bouma G, Strober W. The immunological and genetic basis of inflammatory bowel disease. *Nat Rev Immunol* 2003;**3**:521−33.
2. Malik TA. Inflammatory bowel disease: historical perspective, epidemiology, and risk factors. *Surg Clin* 2015;**95**:1105−22.
3. Kaplan GG. The global burden of IBD: from 2015 to 2025. *Rev Gastro Hepat* 2015;**12**:720−7.
4. Elson CO, Cong Y, McCracken VJ, Dimmitt RA, Lorenz RG, Weaver CT. Experimental models of inflammatory bowel disease reveal innate, adaptive, and regulatory mechanisms of host dialogue with the microbiota. *Immunol Rev* 2005;**206**:260−76.
5. Ko JK, Auyeung KK. Inflammatory bowel disease: etiology, pathogenesis and current therapy. *Curr Pharmaceut Des* 2014;**20**:1082−96.
6. Li H, Fan C, Lu H, Feng C, He P, Yang X, et al. Protective role of berberine on ulcerative colitis through modulating enteric glial cells-intestinal epithelial cells-immune cells interactions. *Acta Pharm Sin B* 2020;**10**:447−61.
7. Peyrin-Biroulet L, Lemann M. Review article: remission rates achievable by current therapies for inflammatory bowel disease. *Aliment Pharmacol Ther* 2011;**33**:870−9.
8. Engel MA, Neurath MF. New pathophysiological insights and modern treatment of IBD. *J Gastroenterol* 2010;**45**:571−83.
9. Shen Z, Zhou Q, Ni Y, He W, Shen H, Zhu L. Traditional Chinese medicine for mild-to-moderate ulcerative colitis: protocol for a network meta-analysis of randomized controlled trials. *Medicine* 2019;**98**. e16881.

10. Cao SY, Ye SJ, Wang WW, Wang B, Zhang T, Pu YQ. Progress in active compounds effective on ulcerative colitis from Chinese medicines. *Chin J Nat Med* 2019;**17**:81−102.

11. Zhang G, Liu M, Song M, Wang J, Cai J, Lin C, et al. Patchouli alcohol activates PXR and suppresses the NF-kappaB-mediated intestinal inflammatory. *J Ethnopharmacol* 2020;**248**:112302.

12. Yu X, Yang G, Jiang H, Lin S, Liu Y, Zhang X, et al. Patchouli oil ameliorates acute colitis: a targeted metabolite analysis of 2,4,6-trinitrobenzenesulfonic acid-induced rats. *Exp Ther Med* 2017;**14**:1184−92.

13. Qu C, Yuan ZW, Yu XT, Huang YF, Yang GH, Chen JN, et al. Patchouli alcohol ameliorates dextran sodium sulfate-induced experimental colitis and suppresses tryptophan catabolism. *Pharmacol Res* 2017;**121**:70−82.

14. Fujiwara N, Kobayashi K. Macrophages in inflammation. *Curr Drug Targets - Inflamm Allergy* 2005;**4**:281−6.

15. Liu YC, Zou XB, Chai YF, Yao YM. Macrophage polarization in inflammatory diseases. *Int J Biol Sci* 2014;**10**:520−9.

16. Zhang J, Zhao Y, Hou T, Zeng H, Kalambhe D, Wang B, et al. Macrophage-based nanotherapeutic strategies in ulcerative colitis. *J Contr Release* 2020;**320**:363−80.

17. Li D, Zhang M, Xu F, Chen Y, Chen B, Chang Y, et al. Biomimetic albumin-modified gold nanorods for photothermo-chemotherapy and macrophage polarization modulation. *Acta Pharm Sin B* 2018;**8**:74−84.

18. Deng N, Li M, Shen D, He Q, Sun W, Liu M, et al. LRP1 receptor-mediated immunosuppression of alpha-MMC on monocytes. *Int Immunopharm* 2019;**70**:80−7.

19. Su Z, Xing L, Chen Y, Xu Y, Yang F, Zhang C, et al. Lactoferrin-modified poly(ethylene glycol)-grafted BSA nanoparticles as a dual-targeting carrier for treating brain gliomas. *Mol Pharm* 2014;**11**:1823−34.

20. Wirtz S, Popp V, Kindermann M, Gerlach K, Weigmann B, Fichtner-Feigl S, et al. Chemically induced mouse models of acute and chronic intestinal inflammation. *Nat Protoc* 2017;**12**:1295−309.

21. Xue F, Wang Y, Zhang Q, Han S, Zhang F, Jin T, et al. Self-assembly of affinity-controlled nanoparticles *via* host-guest interactions for drug delivery. *Nanoscale* 2018;**10**:12364−77.

22. Neudecker V, Haneklaus M, Jensen O, Khailova L, Masterson JC, Tye H, et al. Myeloid-derived miR-223 regulates intestinal inflammation *via* repression of the NLRP3 inflammasome. *J Exp Med* 2017;**214**:1737−52.

23. Yin W, Yu X, Kang X, Zhao Y, Zhao P, Jin H, et al. Remodeling tumor-associated macrophages and neovascularization overcomes EGFRT790M-associated drug resistance by PD-L1 nanobody-mediated codelivery. *Small* 2018;**14**. 1802372.

24. Feng XX, Yu XT, Li WJ, Kong SZ, Liu YH, Zhang X, et al. Effects of topical application of patchouli alcohol on the UV-induced skin photoaging in mice. *Eur J Pharmaceut Sci* 2014;**63**:113−23.

25. Viola A, Munari F, Sanchez-Rodriguez R, Scolaro T, Castegna A. The metabolic signature of macrophage responses. *Front Immunol* 2019;**10**. 1462.

26. Kyriakis JM, Avruch J. Mammalian MAPK signal transduction pathways activated by stress and inflammation: a 10-year update. *Physiol Rev* 2012;**92**:689−737.

27. Schreiber S. Activation of nuclear factor kappa B inflammatory bowel disease. *Gut* 1998;**42**:477−84.

28. Zhou R, Yazdi AS, Menu P, Tschopp J. A role for mitochondria in NLRP3 inflammasome activation. *Nature* 2011;**475**:221−5.

29. Kondylis V, Kumari S, Vlantis K, Pasparakis M. The interplay of IKK, NF-kappaB and RIPK1 signaling in the regulation of cell death, tissue homeostasis and inflammation. *Immunol Rev* 2017;**277**:113−27.

30. Pedros C, Duguet F, Saoudi A, Chabod M. Disrupted regulatory T cell homeostasis in inflammatory bowel diseases. *World J Gastroenterol* 2016;**22**:974−95.

31. Liu H, Hu B, Xu D, Liew FY. CD4$^+$CD25$^+$ regulatory T cells cure murine colitis: the role of IL-10, TGF-beta, and CTLA4. *J Immunol* 2003;**171**:5012−7.

32. Stagg AJ, Hart AL, Knight SC, Kamm MA. The dendritic cell: its role in intestinal inflammation and relationship with gut bacteria. *Gut* 2003;**52**:1522−9.

33. Zhang R, Yan P, Li Y, Xiong L, Gong X, Peng C. A pharmacokinetic study of patchouli alcohol after a single oral administration of patchouli alcohol or patchouli oil in rats. *Eur J Drug Metab Pharmacokinet* 2016;**41**:441−8.

34. Wang HT, Wang ZZ, Wang ZC, Wang SM, Cai XJ, Su GH, et al. Patchouli alcohol attenuates experimental atherosclerosis *via* inhibiting macrophage infiltration and its inflammatory responses. *Biomed Pharmacother* 2016;**83**:930−5.

35. Yu Y, Zhang Y, Wang S, Liu W, Hao C, Wang W. Inhibition effects of patchouli alcohol against influenza a virus through targeting cellular PI3K/Akt and ERK/MAPK signaling pathways. *Virol J* 2019; **16**. 163.

36. Xu YF, Lian DW, Chen YQ, Cai YF, Zheng YF, Fan PL, et al. *In vitro* and *in vivo* antibacterial activities of patchouli alcohol, a naturally occurring tricyclic sesquiterpene, against *Helicobacter pylori* infection. *Antimicrob Agents Chemother* 2017;**61**. e00122-17.

37. Gren ST, Grip O. Role of Monocytes and intestinal macrophages in Crohn's disease and ulcerative colitis. *Inflamm Bowel Dis* 2016;**22**: 1992−8.

38. Jin K, Luo Z, Zhang B, Pang Z. Biomimetic nanoparticles for inflammation targeting. *Acta Pharm Sin B* 2018;**8**:23−33.

39. Xian X, Ding Y, Dieckmann M, Zhou L, Plattner F, Liu M, et al. LRP1 integrates murine macrophage cholesterol homeostasis and inflammatory responses in atherosclerosis. *Elife* 2017;**6**. e29292.

40. Mueller PA, Zhu L, Tavori H, Huynh K, Giunzioni I, Stafford JM, et al. Deletion of macrophage low-density lipoprotein receptor-related protein 1 (LRP1) accelerates atherosclerosis regression and increases C−C chemokine receptor type 7 (CCR7) expression in plaque macrophages. *Circulation* 2018;**138**:1850−63.

41. Danhier F. To exploit the tumor microenvironment: since the EPR effect fails in the clinic, what is the future of nanomedicine?. *J Contr Release* 2016;**244**:108−21.

42. Chen Q, Xiao B, Merlin D. Nanotherapeutics for the treatment of inflammatory bowel disease. *Expet Rev Gastroenterol Hepatol* 2017; **11**:495−7.

43. Talekar M, Tran TH, Amiji M. Translational nano-medicines: targeted therapeutic delivery for cancer and inflammatory diseases. *AAPS J* 2015;**17**:813−27.

44. Binion DG, Rafiee P. Is inflammatory bowel disease a vascular disease? Targeting angiogenesis improves chronic inflammation in inflammatory bowel disease. *Gastroenterology* 2009;**136**:400−3.

45. Nunes R, Neves JD, Sarmento B. Nanoparticles for the regulation of intestinal inflammation: opportunities and challenges. *Nanomedicine* 2019;**14**:2631−44.

46. Watanabe A, Tanaka H, Sakurai Y, Tange K, Nakai Y, Ohkawara T, et al. Effect of particle size on their accumulation in an inflammatory lesion in a dextran sulfate sodium (DSS)-induced colitis model. *Int J Pharm* 2016;**509**:118−22.

47. Na YR, Stakenborg M, Seok SH, Matteoli G. Macrophages in intestinal inflammation and resolution: a potential therapeutic target in IBD. *Rev Gastroenterol Hepatol* 2019;**16**:531−43.

48. Rogler G, Brand K, Vogl D, Page S, Hofmeister R, Andus T, et al. Nuclear factor kappaB is activated in macrophages and epithelial cells of inflamed intestinal mucosa. *Gastroenterology* 1998;**115**: 357−69.

49. Choi YH, Bae JK, Chae HS, Choi YO, Nhoek P, Choi JS, et al. Isoliquiritigenin ameliorates dextran sulfate sodium-induced colitis through the inhibition of MAPK pathway. *Int Immunopharm* 2016;**31**: 223−32.

50. Joh EH, Kim DH. Kalopanaxsaponin A ameliorates experimental colitis in mice by inhibiting IRAK-1 activation in the NF-kappaB and MAPK pathways. *Br J Pharmacol* 2011;**162**:1731−42.